Light-Scattering Study of DNA Condensation: Competition Between Collapse and Aggregation

CAROL BETH POST* and BRUNO H. ZIMM, *Department of Chemistry, B-017, University of California at San Diego, La Jolla, California 92093*

Synopsis

Light-scattering studies were done to investigate the DNA collapse transition, a large and discontinuous reduction in the radius of gyration. Of particular concern was differentiating the compaction of a single DNA molecule from aggregation. Solutions of RK2 plasmid DNA ($M_r = 37 \times 10^6$) or bacteriophage T7 DNA ($M_r = 25 \times 10^6$) were titrated with the condensing reagents spermidine in aqueous solvent or magnesium ion in ethanol–water solvent. The transition was followed by the change in scattering at a single angle or by the change in the angular dependence of scattering. At concentrations below 1 μg/mL, only aggregation could be detected by observation at a single angle; therefore, to study the collapse transition, it was necessary to measure the angular dependence of scattering. The intensities measured between the angles 30° and 60° were fit to known scattering functions. At low concentrations of the condensing reagent, the data were consistent with the scattering function of a random coil. On the other hand, during the transition at higher reagent concentrations, the curve that fit the data required two components—the scattering function for a random coil with a large radius of gyration, plus that for a sphere with a radius about one-fifth of that of the coil. The fractional concentration of the sphere increased with increasing condensing-reagent concentration. This two-component behavior is in apparent contrast to the situation with a more flexible polymer such as polystyrene, in accord with theoretical predictions. At still higher reagent concentrations, aggregation was apparent. Condensation to a collapsed state was reversible without hysteresis, while dissolution of the aggregated state nearly always occurred with hysteresis. Qualitative agreement between the observed DNA collapse transition and the theoretical phase diagram presented in the preceding paper was found, although the light-scattering results did not show quantitative agreement with the simple theoretical model.

INTRODUCTION

The theoretical phase diagram of a DNA solution, reported in the preceding paper,[1] discriminates between two mechanisms of DNA condensation in a poor-solvent environment: (1) the compaction or collapse of a single DNA molecule at very dilute DNA concentrations and (2) the aggregation of many molecules at higher DNA concentrations. The intent of this work is to distinguish experimentally the two mechanisms of condensation using static light scattering. Study of the collapse transition of a polymer with high-molecular-weight DNA is advantageous because DNA is monodisperse and is rigid enough that a discontinuous change in

* Present address: Inorganic Chemistry Laboratory, Oxford, England OX1 3QR.

Biopolymers, Vol. 21, 2139–2160 (1982)

CCC 0006-3525/82/112139-22$03.20

the radius of gyration, R_g, is predicted.[2] Light scattering is a reasonable method to study the collapse transition because the substantial reduction in R_g in the compact form leads to a large increase in the scattered intensity. Moreover, light scattering allows an evaluation of the molecular weight, and thus a distinction can be made between the concentrated aggregated phase and the dilute single-molecule collapsed phase. That a monomolecularly collapsed, thermodynamically stable state of DNA exists has not been shown by previous studies. Although the compaction of DNA, as evidenced by an increase in the translational diffusion coefficient[3,4] and the loss of deformability of DNA in flow,[5] has been demonstrated, prior observations could not rule out any change in the molecular weight, M_r, of the stable phase upon condensation.

The work reported here involved measuring the changes in scattered intensities when solutions of T7 and RK2 DNA were titrated with condensing reagents. Initially, it was hoped that the coexistence curve[1] could be mapped as a function of DNA concentration by monitoring the change in light scattering at a single angle. The biphasic region and the collapse region would be distinguished by their different dependences on the DNA concentration. There is a negative slope to the part of the curve dividing the expanded state from the biphasic region; thus, separation into two phases, detected by a sudden rise in the scattering, should occur at a lower concentration of condensing reagent (a lower χ value) for a larger DNA concentration. In contrast, transition from the expanded coil to the monomolecular, collapsed state should be independent of DNA concentration.

The transition was, in fact, found to occur with very little DNA concentration dependence at all concentrations investigated; thus, the measurement at a single angle is insufficient to distinguish aggregation from a mononuclear collapse. Measurements over a range of angles were therefore made to investigate the change in M_r and R_g with added condensing reagent. We found that the angular dependence of the scattered intensity during the transition to a condensed state cannot be fit with a single scattering function, but that the data are consistent with a sum of two scattering functions: the function for a random coil with a large R_g and the function for a sphere with a small R_g. The fractional amount of scattering contributed by the sphere increased with an increase in the concentration of condensing reagent.

We also investigated the reversibility of the transition. The results indicate that dissolution of the aggregated state occurs with hysteresis but that the unfolding of the collapsed state can happen without hysteresis.

This study elucidates neither the specific forces involved in the mechanism of compaction nor the helical organization of folding in the collapsed state. Before one can investigate the details of the solution structure, one must establish the experimental conditions that produce a stable compact form.

MATERIALS AND METHODS

Light-Scattering Apparatus and Measurements

The light-scattering apparatus was built in this laboratory and has been described in detail.[6,7] A Spectra-Physics model 120, 5-mw, He-Ne laser operating at 632.8 nm serves as a light source. The instrument was calibrated with filtered benzene and carbon tetrachloride. Since the cell holder was filled with water during the calibration, a correction for the difference in the refractive index of the organic solvent and that of water was applied. Relating the instrumental reading at 90° to the literature value[8] for the Rayleigh ratio determines a cell constant. Cell constants evaluated from the two solvents and from different samples of the same solvent agreed within approximately 10%. The variation of reflectivity of the cell surface with observation angle was assumed to be less than 15% and was neglected. Light-scattering measurements were made at room temperature, ~21°C.

Sample Preparation

Solution Clarification

Buffer solutions were filtered several times through Millipore filters, type GS, 0.22μ. Aqueous buffers were filtered by vacuum, and ethanol–water solutions were filtered under pressure. All glassware was extensively rinsed with filtered solutions. DNA stock solutions were not filtered. Dilution of the DNA stock into the sample was high enough that the small amount of dust transferred with the DNA was tolerable in most cases. Before each experiment, samples were checked for clarity by examination by eye at very low angles and by measurement of solvent background scattering and were discarded if the background noise was too high.

DNA Purification

E. coli B was grown in Luria broth to about 5×10^8 cells/mL and infected with T7 bacteriophage. Immediately before lysis by the phage, the cells were concentrated by centrifugation and lysed with chloroform. T7 phage was banded by CsCl density-gradient centrifugation. T7 DNA ($M_r = 25 \times 10^6$) was purified by the hot phenol extraction method.[9] After the DNA phase was clear, usually requiring three to four extractions, the phenol was removed from the DNA solution by dialysis against either phosphate buffer (0.008M PO_4^{2-}, 0.016M Na^+, 0.001M EDTA, pH 6) or cacodylate buffer (0.001M sodium cacodylate, 0.015M NaCl, 0.01 mM EDTA, pH 6). The DNA stock solution was stored at 4°C.

E. coli C600 containing plasmid RK2 with a gift from the lab of D. Helinski. *E. coli* was grown on Luria broth overnight. The cells were concentrated and lysed with lysozyme and 2% sodium *N*-lauroylsarcosinate.

Plasmid DNA, $M_r = 37 \times 10^6$ (Kolter et al.[10]) was purified by ethidium bromide–CsCl density-gradient centrifugation and was linearized by cutting with EcoR1 at the single sensitive site. The DNA stock solution was dialyzed against cacodylate buffer (0.01*M* sodium cacodylate, 0.005*M* NaCl, 0.5 m*M* Na_2 EDTA, pH 7).

The DNA concentration of stock solutions was determined by absorption at 260 nm in 1-cm cells with an absorbance coefficient of 55 μg/mL-unit absorbance.

Solutions

Light-scattering samples were buffered by cacodylate: 0.001*M* for spermidine condensation and 0.010*M* for condensation in ethanol–water solutions. NaCl was added to attain the specified Na^+ concentration. The concentration of Mg^{2+} in the magnesium acetate stock solution was determined by conductance measurements, using solution conductivities from *The International Critical Tables.*[11] Spermidine was purchased from Sigma and purified by ionic-exchange chromatography using BioRad AG5O-X2 resin, 100–200 mesh, followed by cold recrystallization in acidic ethanol–water solution.[12] Such purification is important since the presence of small amounts of higher amines, such as spermine, can markedly affect DNA condensation. Solutions containing ethanol were made by weight to circumvent possible errors due to volume changes upon mixing and were kept tightly covered whenever possible to avoid evaporation of ethanol.

To achieve reproducible critical concentrations in the reagent inducing condensation (spermidine, ethanol, or Mg^{2+}), it was necessary to maintain carefully the concentrations of other solvent constituents (Na^+, Mg^{2+}, and ethanol). Several workers[13–16] have discussed the strong interdependence of the environmental effects that promote condensation (e.g., total concentration of all counterions, the dielectric constant of the solvent, temperature, pH). The interdependence of the concentrations of ethanol and magnesium ion found in this study is discussed below.

Sample Mixing

Dilution buffers and the DNA stock were pipetted directly into the scattering cell and then mixed by gently inverting the cell several times. Titration of the sample was done by adding small aliquots of a condensing reagent to the cell and again inverting to mix the solution.

RESULTS

Scattering at 90°

The simplest approach to observing the collapse transition by light scattering is to measure the scattering at a single angle as the condensing reagent is added.[3,16] Such a curve of intensity versus amount of condensing

reagent shows very little scattering until a sudden sharp rise occurs at a critical concentration of condensing reagent. It is tempting to identify this rise with the onset of collapse. (As the molecule collapses, the phase difference between the rays scattered from different parts of the molecule becomes less and the intensity of the scattering increases.) Unfortunately, aggregation of the DNA also causes the scattering to increase, and it is not always easy to distinguish the two effects with measurements at only one angle. It is possible to set limits on the extent of the increase that can result from collapse, however, as described below. Also, in principle the two processes should be distinguishable through their concentration dependences, since aggregation should depend on the DNA concentration whereas collapse should not.[1]

The scattered intensity from a solution of unaggregated molecules cannot be greater than that allowed by the familiar equation:

$$K\frac{c}{R_\theta} = \frac{1}{M_r P(\theta)} + 2A_2 c \tag{1}$$

with the optical constant

$$K = \left[2\pi\tilde{n}\left(\frac{\partial\tilde{n}}{\partial c}\right)\right]^2 \Big/ N_A\lambda_0^4 \tag{2}$$

R_θ is the Rayleigh ratio (the intensity of scattered light at the angle θ relative to that of the incident beam), c is the DNA concentration in g/mL, and M_r is the DNA molecular weight. K is equal to 1.99×10^{-7} for the following values of the parameters: the refractive index for both aqueous solvent and, in approximation, for the mixed ethanol–water solvent, $\tilde{n} = 1.33$; the refractive index increment for DNA,[17] $\partial\tilde{n}/\partial c = 0.166$; the light wavelength, $\lambda_0 = 632.8$ nm. No significant error would be introduced into the analysis of the light-scattering data from the mixed solvent if there was a preferential adsorption of water to the DNA, since the refractive indexes of water and ethanol are very close ($\tilde{n}$ equals 1.33 and 1.36 for water and ethanol, respectively). To set limits on the increase in scattering due to collapse, the viral term in Eq. (1) is assumed to be negligible, since both the collapse transition and aggregation occur close to the Flory θ-point where A_2 equals zero. The maximum possible value of the scattering intensity, R_θ, can be calculated from the known value for M_r and the assumption that $P(\theta)$ is unity. Actually, $P(\theta)$ cannot be greater than unity and is probably less [$P(\theta)$ is strictly equal to unity only at θ equal to 0°, as discussed in the following section]; hence, this calculated R_θ is a maximum intensity. Then, if the measured R_θ were greater than that calculated, the sample must have had M_r greater than the monomolecular value.

A few results of this kind from RK2 DNA are shown in Table I. The structural transition was induced in mixed ethanol–water solvents both by titration with magnesium ion at a constant ethanol concentration and by titration with ethanol at a constant magnesium concentration. The reported c/R_θ values were calculated from the intensities measured after

TABLE I
Magnesium Concentration at the Transition of the 90° Scattering Intensity as a Function of RK2 DNA Concentration[a]

[DNA] (μg/mL)	log[DNA]	[Ethanol] (%, w/w)	[Mg^{2+}] (mM)	$c/R_{90°}$ [b]
0.3	−0.52	26	4.5[c]	0.54
			4.6	0.04
0.5	−0.30	26	4.0[c]	0.76
			4.3	0.11
1.0	0.00	26	4.0[c]	0.76
			4.3	0.10
2.9	0.46	26	4.1[c]	1.20
			4.3	0.07
1.6	0.20	10.6[d]	50	1.01
		11.7		0.04
4.9	0.69	10.4[d]	50	3.27
		11.8		0.05

[a] Mixed ethanol–water solvent. [Na^+] = 0.011M.

[b] Aggregation is indicated by a measured value of c/R_θ less than 0.14, the calculated value for monomolecular RK2 DNA at zero angle.

[c] The step in magnesium concentration at which aggregation occurs.

[d] The step in ethanol concentration at which aggregation occurs.

the scattering had stabilized at the given solvent conditions. For $M_r = 37 \times 10^6$ for RK2 DNA, the minimum value for c/R_θ is 0.14; anything less than this must indicate aggregation. Examination of the data in Table I shows that the scattering jumps from a very low intensity (the first point of each pair) to a value indicative of aggregation (the second point of each pair). Even at the lowest DNA concentration (0.3 μg/mL), the transition observed at 90° indicated aggregation, since the abrupt rise in the intensity was to a level too high to be the result of a conformational change of only one DNA molecule. With small additions of the condensing reagent, the intensity continued to increase to levels much greater than those shown in Table I. (As well as aggregation, it must be recognized that a negative A_2 can also result in an intensity greater than the single-molecule zero-angle scattering. Nonetheless, even a negative value for A_2 as large in magnitude as 22×10^{-4} mol mL/g^2, the maximum positive value reported by Borochov et al.,[18] cannot account for the observed increase in scattering.)

The concentrations of Mg^{2+} and ethanol that produce the structural transition of DNA are interdependent, a higher Mg^{2+} concentration being required with a lower percent ethanol (see Table I).

We had hoped to be able to distinguish aggregation from collapse by the dependence on DNA concentration of the point of rapid rise of scattering, since collapse should be independent of concentration, in contrast to aggregation. The data showed, however, that not only was aggregation the one transition detected by the single-angle measurement, but that the dependence of the point of aggregation on DNA concentration was too slight to be useful for making this distinction.

Similar results were obtained in a titration with spermidine over a range of DNA concentrations from 0.4 to 3.2 μg/mL (results not shown). It was not feasible to go to lower concentrations in either titration because the rise above the background of the scattering upon titration became too small to measure reliably before aggregation appeared. It seems likely to us that aggregation was present in all previously reported titrations of this kind that used conventional light scattering as the means of detection.

Angular Dependence of the Scattering Intensity

Monitoring of the scattering intensity at a single angle did not give evidence of a single-molecule collapsed state; therefore, a more thorough examination of the conformational changes of DNA was pursued. It was necessary to determine the change in M_r and R_g with added condensing reagent to differentiate the collapse transition from aggregation. Estimates of M_r and R_g were obtained from the angular dependence of scattering over the angular range of 30°–60°. These quantities were not established with high accuracy because of the low DNA concentration and because the angles were high; nonetheless, the measurements were sufficient to characterize qualitatively the gross structural transition resulting from a change in the solvent conditions.

The angular-dependence measurements were done by Mg^{2+} titration of RK2 DNA in ethanol–water solutions. A very slow rate of titration was used for these experiments. Solutions were left at a given collapsing-reagent concentration until the intensity level was stable. This incubation period was commonly 2 h, and sometimes as long as 25 h.

Determination of M_r and R_g requires knowing the effects of interference in the scattering from particles whose size approximates the light wavelength as expressed in the scattering function $P(\theta)$. $P(\theta)$ is the ratio of the intensity scattered through the angle θ to that scattered without phase change, i.e., through zero angle, and is calculated from the spatial distribution of scattering elements within the particles. The general equation for $P(\theta)$ includes a sum over μr_{ij}, where r_{ij} is the vector distance between elements and

$$\mu = 4\pi/\lambda \sin(\theta/2) \tag{3}$$

λ is the wavelength of scattered light in the medium ($\lambda = \lambda_0/\tilde{n}$).

In the limit as θ approaches 0°, $P(\theta)$ becomes independent of molecular shape and is related to the square of the radius of gyration, R_g^2, by

$$\lim_{\theta \to 0} P^{-1}(\theta) = 1 + \frac{16\pi^2}{3\lambda^2} R_g^2 \sin^2\left(\frac{\theta}{2}\right) + \cdots \tag{4}$$

M_r, R_g, and A_2 are typically determined from light-scattering data by evaluation of the intercept and limiting slopes on a reciprocal-intensity plot[19] [see Eq. (1)]. This procedure is valid only for values of $P^{-1}(\theta)$ close to 1.0, where the reciprocal-intensity plotted against $\sin^2(\theta/2)$ is essentially

linear.[17,19,20] At large values of θ and R_g, there is curvature in $P^{-1}(\theta)$, specific to the molecular form, and extrapolation from a high θ region to zero angle does not give the true initial slope and intercept. Given the high molecular weight of the DNA and the angular range of 30°–60° used in this work, $P^{-1}(\theta)$ is significantly greater than the limiting value. Therefore, M_r and R_g cannot be obtained directly from the limiting slope and intercept of a straight-line plot. A more appropriate procedure is to fit the data to a theoretical curve of the scattering intensity as a function of angle, calculated from an assumed $P(\theta)$ with given values of the parameters.

A. Random-Coil State at Low Magnesium Concentration

The scattering measured at low Mg^{2+} concentrations was compared with the theoretical $P(\theta)$ for a random coil. Although DNA is best modeled using wormlike chain statistics, the large size of RK2 DNA (270–380 persistence lengths per molecule) makes approximation as a random coil possible without substantial error. Excluded-volume effects are significant for the low-salt conditions (0.011*M* NaCl) present at the beginning of the Mg^{2+} titration and are considered in this analysis.

The scattering function for a random coil without excluded volume is expressed as

$$P_{RC}(\theta) = (2/u^2)(e^{-u} + u - 1) \tag{5}$$

$$u = \mu^2 R_g^2 \tag{6}$$

The scattering function for a random coil with excluded volume was obtained from Fig. 2 of Sharp and Bloomfield.[21] Only the $P(\theta)$ curves for which the excluded-volume parameter, ϵ, is less than 0.2 were considered. This upper limit for ϵ is based on reports in the literature on excluded-volume measurements in aqueous solvent. For 0.01*M* Na^+, these values are $\epsilon = 0.16$, as measured by Borochov et al.,[18] and $\epsilon = 0.18$, as measured by Ross and Scruggs.[22]

The data were fit to the plot of $P_{RC}^{-1}(\theta)$ versus u. The observed intensities are related to $P^{-1}(\theta)$ by Eq. (1). A_2 is set equal to zero, since, in the low-intensity region of $P^{-1}(\theta)$ being considered, the virial term in the equation is negligible. The known value for M_r of 37×10^6 was assumed, as it was whenever the observed intensity at all angles was below the expected zero-angle intensity. The measured intensities were fit to the slope and to the scattering level of the theoretical curve by adjusting the values of R_g and ϵ. A decrease in R_g results in smaller u values for a given displacement along the ordinate and in an increase in the slope. Because of the low DNA concentration used in this work, a reliable determination of R_g and ϵ was not possible. The data can only specify a range of values for R_g consistent with $\epsilon < 0.2$. Although an absolute value for ϵ is not known, ϵ is at its maximum for the titration when $[Mg^{2+}] = 0$, decreases with the addition of Mg^{2+}, and is very close to 0.0 at the phase-transition point. Examples of data fit to the theoretical curves using several possible values of R_g and

ϵ are shown in Fig. 1. In Fig. 1(a) the data points correspond to the intensities measured between 30° and 60° for RK2 DNA (5μg/mL and Mg^{2+} = 0) and are compared to the theoretical curves for $P_{RC}^{-1}(\theta)$ plotted against u, with ϵ equal to 0.0, 0.1, and 0.2. Three possible fits are shown for R_g equal to 800, 950, and 975 nm. Agreement between the observed intensities and the theoretical curves can also be confirmed by referring to the more familiar reciprocal-intensity plot. The same data are plotted as c/R_θ against $\sin^2(\theta/2)$ in Fig. 1(b), along with the theoretical curves for two values of R_g and ϵ.

B. Condensed State at Intermediate Magnesium Concentration

The angular dependence of the scattering from samples with Mg^{2+} concentrations aproximately 3.3 to 3.6 mM and greater did not follow the dependence expected for randomly coiled molecules. The angular dependence was small, yet the reciprocal intensities were too high to be the result of a collapsed coil with a small R_g. While the reciprocal intensity at the higher angles decreased somewhat compared to samples with [Mg^{2+}] < 3.3 mM, the reciprocal intensity at the lower angles remained relatively high, such that the plot required substantial curvature to pass through the expected intercept. An example of data that do not follow a random-coil scattering function is shown in Fig. 2. No adjustment of R_g or ϵ allows a satisfactory fit to the theoretical curves, nor would a reasonable change in M_r allow a fit, a smaller value of M_r being required.

A composite scattering function is necessary to match the observed reciprocal intensities under these conditions. The total $P(\theta)$ is expressed as a sum of two functions, with each $P(\theta)$ function multiplied by the fraction of the total DNA concentration existing in the molecular shape specified by $P(\theta)$, as is shown by Eq. (7) below. The solvent conditions being considered are very close to those at the point of a phase transition (collapse or aggregation), so both ϵ and the second virial coefficient, A_2, are assumed to equal zero. The parameter f is the fraction of DNA in the expanded, randomly coiled configuration and c_0 is the total concentration of added DNA. From Eq. (1),

$$R_\theta = KM_r c_0[fP_{RC}(\theta) + (1 - f)P_2(\theta)] \tag{7}$$

A characteristic of $P_2(\theta)$ required to fit the data is a smaller angular dependence than that of a random coil with a large R_g; the scattering function of a sphere with a small radius R is suitable and was the function used. This function is

$$P_S(\theta) = \left(\frac{3}{x^3}(\sin x + x \cos x)\right)^2 \tag{8}$$

$$x = \mu R \tag{9}$$

[The fit using $P_S(\theta)$ is probably not unique. Another possible model would have each molecule partially collapsed and partially expanded. Never-

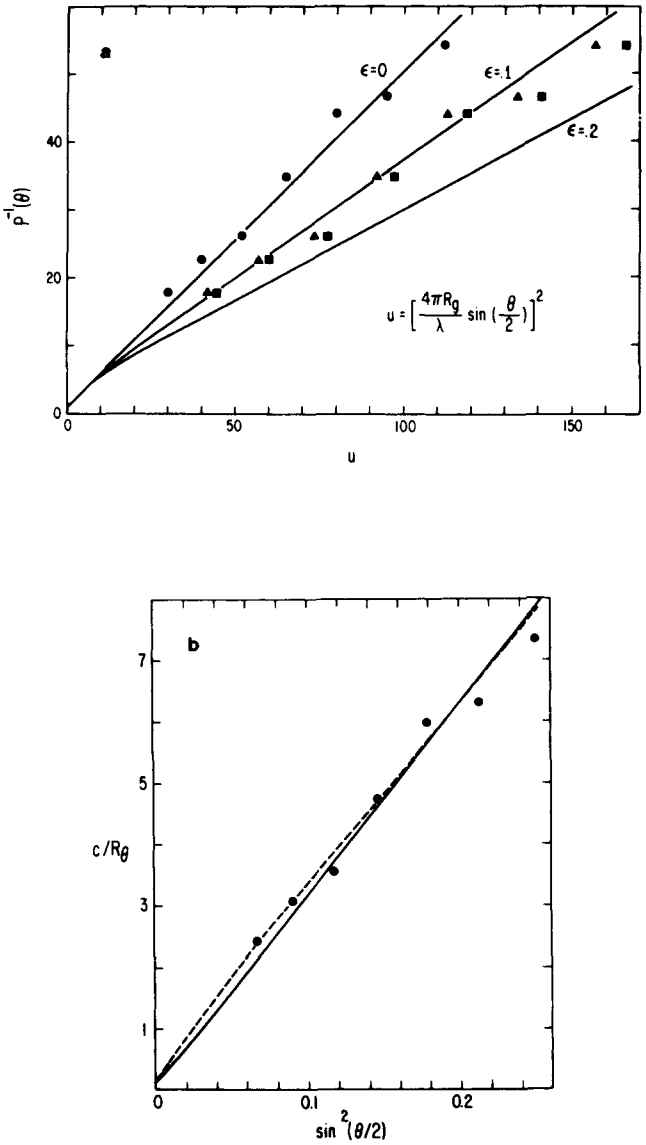

Fig. 1. (a) Light-scattering data of RK2 DNA in ethanol–water solvent, without magnesium, compared to the reciprocal of the scattering function, $P^{-1}(\theta)$, for an extended random coil with excluded volume. The theoretical curve for the excluded-volume parameter, ϵ, equal to 0.0 is calculated from Eq. (5), and those for ϵ equal to 0.1 and 0.2 are from Fig. 2 of Sharp and Bloomfield (Ref. 21). The data are for RK2 DNA, 5 μg/mL, 25% by weight ethanol, 0.011M Na^+, $[Mg^{2+}] = 0$. Ordinate values of the data are determined from $P^{-1}(\theta) = cKM_r/R_\theta$ for $M_r = 37 \times 10^6$. The value of u depends on θ and R_g. Data are plotted for three radii of gyration: (●) R_g = 800 nm; (▲) R_g = 950 nm; (■) R_g = 975 nm. (b) Reciprocal-intensity plot of the same data shown in (a) compared to theoretical curves for an extended random coil. The curves were calculated for $M_r = 37 \times 10^6$, with (—) P_{RC} taken from Eq. (5) for $\epsilon = 0$, R_g = 810 nm and (- - -) P_{RC} taken from Fig. 2 of Sharp and Bloomfield[21] for $\epsilon = 0.1$, R_g = 950 nm.

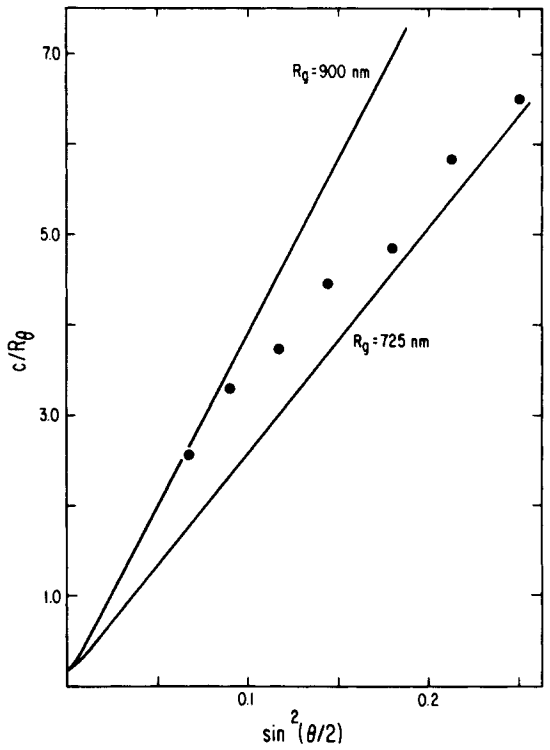

Fig. 2. Light-scattering data of RK2 DNA in ethanol–water solvent with magnesium compared to theoretical reciprocal-intensity curves for extended random coil. The curves are calculated for $M_r = 37 \times 10^6$, and $R_g = 900$ (left) and 725 nm (right). The data points were measured for RK2 DNA, 9.9 μg/mL, 25% by weight ethanol, 11 m*M* Na^+, 3.6 m*M* Mg^{2+}. No agreement of the data with the random-coil scattering function is possible.

theless, all the data were compatible with $P_2(\theta)$ in Eq. (7) being that of a sphere; thus, the only model considered in this report is that each molecule is either an expanded coil or a compact sphere.]

In fitting the observed angular dependence of the scattering at a given Mg^{2+} concentration to Eq. (7), M_r is set equal to 37×10^6 whenever the observed intensity is less than the expected zero-angle intensity. Values were determined for $P_{RC}(\theta)$ from Eq. (5) with R_g varying between 550 to 975 nm, and for $P_S(\theta)$ from Eq. (8) with R varying between 50 and 175 nm. For a given pair, R_g and R, the fraction of the total intensity attributed to $P_{RC}(\theta)$ was evaluated from the intensity, R_θ, measured at each angle θ using Eq. (7). The parameter f was then calculated from the average over θ, as given by

$$f = \frac{1}{N} \sum_{i=1}^{N} \frac{(R_{\theta_i}/cKM_r) - P_S(\theta_i)}{P_{RC}(\theta_i) - P_S(\theta_i)} \tag{10}$$

The best agreement between the data and the theoretical predictions was achieved by minimizing the sum over all θ of the squared deviations between

the observed and calculated values. Minimization of the differences was done both with the intensities and with the reciprocal intensities. R_g and R corresponding to the minimum were generally equivalent for either summation variable, with only small variations occurring in some cases. Some samples did not have a strong minimum, and the data could be matched, within experimental error, by theoretical curves evaluated with a wide range of values for f, R_g, and R. In particular, the calculated intensities fit to solutions for which more than 10% of the scattering appears to result from condensed spherelike particles ($f < 0.9$) were insensitive to R_g, and very little change in the sum of squared deviations was found for any value of R_g between 550 and 975 nm. Examples of data fit using the composite function are shown in Fig. 3. The data include those in Fig. 2.

C. Aggregated State at High Magnesium Concentration

Samples for which the scattered intensity at finite angles is much greater than that expected for monomolecular DNA at zero angle are certainly aggregated. The data approximate the scattering function for a sphere, with a reasonable fit obtained by varying R and by using $M_r > 37 \times 10^6$.

D. Sizes and Amounts of the Two Components

R_g, R, and f evaluated for RK2 DNA, ranging in concentration from 0.3 to 9.9 μg/mL, in mixed solvent at different Mg^{2+} concentrations, are given in Table II. Parentheses around R_g indicate that the minimization was not sensitive to the R_g value in this particular case, as discussed in section B.

For $[Mg^{2+}] < 3.6$ mM, the scattering intensities from samples of RK2 DNA in ethanol–water solvents were fit by $P_{RC}(\theta)$ with R_g between 725 and 975 nm. We also measured the scattering from RK2 DNA in aqueous solution without ethanol (Table III). Since all solutions were rather dilute (<10 μg/mL), the accuracy of the data do not allow a unique determination of R_g and ϵ, as stated in Section A. The R_g values reported here are somewhat larger than the value of 740 nm determined by Ross and Scruggs[22] from the intrinsic viscosity of sheared T4 DNA ($M_r = 39 \times 10^6$). The discrepancy is not large and is thought to be within the limit of experimental and theoretical uncertainty. Comparison of the results in Table III with those in Table II obtained at low Mg^{2+} concentrations finds that there is no detectable effect on R_g of the mixed solvent alone.

Furthermore, in the absence of ethanol, the angular dependence of scattering could be fit with $P_{RC}(\theta)$ at all Mg^{2+} concentrations investigated, with no evidence of collapse or aggregation. In mixed solvent, however, the second component of smaller dimension and less angular dependence in scattering had to be included when $[Mg^{2+}]$ was greater than 3.6 mM. The data are consistent with a solution composed of a mixture of random

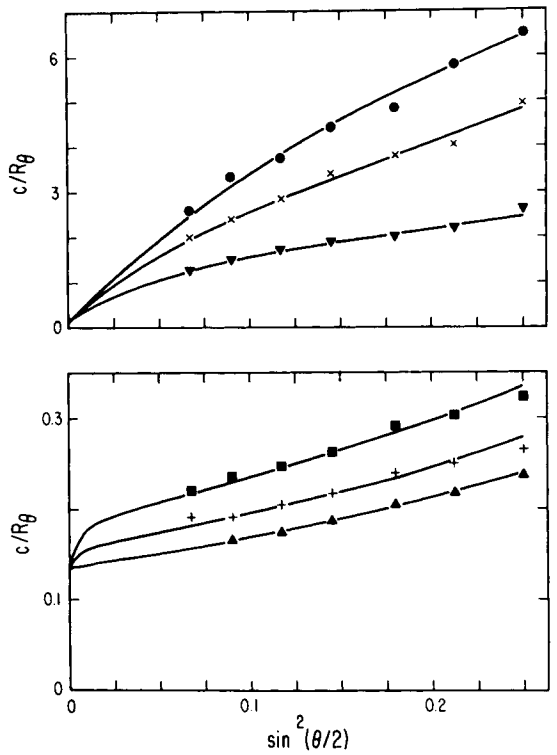

Fig. 3. Reciprocal-intensity plot of the scattering data from RK2 DNA fit with two scattering functions. RK2 DNA, 9.9 μg/mL, 25% by weight ethanol, 11 mM Na^+. The total scattering as a function of angle is a sum of fP_{RC}, for a random coil with dimension R_g, plus $(1-f)P_S$, for a sphere with radius R, with f the fraction of DNA in a random-coil configuration. All curves are calculated using $M_r = 37 \times 10^6$. Symbols are as follows:

	$[Mg^{2+}]$	f	R_g	R
●	3.6 mM	0.99	975 nM	75 nM
×	4.0	0.97	950	125
▼	4.3	0.94	850	100
■	4.6	0.30	800	125
+	4.7	0.14	800	125
▲	4.9	0.00	—	125

coils and spheres, the latter with a radius between 50 and 175 nm, with 125 nm found most often. (The fraction of the volume of the sphere occupied by the DNA is still less than 0.1, even at the minimum radius measured.) As the Mg^{2+} concentration in the mixed solvent increased, the fractional amount of scattering contributed by the condensed spheres increased.

Titration of some DNA solutions to a still higher Mg^{2+} concentration induced the formation of aggregates of large M_r but rather small in size under the conditions observed.

When the DNA concentration was less than 2 μg/mL, the angular dependences could not be measured at low Mg^{2+} levels because of the small

TABLE II
Parameters Fit to the Light-Scattering Data of RK2 DNA as a Function of Magnesium Concentration[a]

[RK2 DNA] (μg/mL)	[Mg^{2+}] (mM)	[Mg^{2+} – EDTA] (mM)	f	R_g [b] (nm)	R (nm)	$M_r \times 10^{-6}$
0.3	4.3		0.29	(600)	150	37
	4.5		0.27	(675)	150	37
	4.6		0.00		125	270
0.5	4.24		0.38	600	125	37
	4.31		0.23	(600)	125	37
	4.37		0.15	(600)	125	37
0.6	4.3		0.80	(975)	125	37
	4.9		0.45	(600)	175	37
	5.2		0.00		150	160
2.0	4.0		0.93	975	125	37
	4.3		0.89	750	175	37
		4.5	0.87	(975)	150	37
	4.6		0.93	(700)	50	37
		4.7	0.77	(875)	125	37
	4.9		0.68	(600)	75	37
		4.9	0.55	(975)	100	37
	5.2		0.41	(600)	75	37
5.0	0		1.00	800–975[d]		37
	3.3		1.00	675–725[d]		37
	3.6		0.98	825	50	37
	3.8		0.95	925	150	37
	4.0		0.94	850	175	37
		4.0	0.96	750	175	37
	4.3		0.96	775	125	37
		4.3	0.96	825	150	37
	4.6		0.94	625	50	37
		4.7[c]	0.00		125	65.5
9.9	0		1.00	875–975[d]		37
	3.6		0.99	975	75	37
	4.0		0.97	950	125	37
		4.2	0.97	800	175	37
	4.3		0.94	850	100	37
	4.6		0.30	(800)	125	37
		4.6	0.40	(550)	150	37
	4.7		0.14	(800)	125	37
	4.9		0.00		125	37

[a] Ethanol concentration, 25% by weight. Mixed ethanol–water solvents, [Na^+] = 0.011M. f, fraction of DNA in random coil; R_g, random-coil radius of gyration; R, sphere radius.

[b] The values of R_g in parentheses are not known with certainty since the fit to the data was not sensitive to R_g.

[c] Data are also consistent with $f = 0$, $R = 100$ nm, $M_r = 37 \times 10^6$, and $A_2 = -11.9 \times 10^{-4}$ mol mL/g^2.

[d] The range in R_g corresponds to a range in the excluded-volume parameter, $0 < \epsilon < 0.2$.

TABLE III
Parameters Fit to the Light-Scattering Data of RK2 DNA in Aqueous Solvent as a Function of Magnesium Concentration[a]

$[Mg^{2+}]$ (mM)	R_g [b] (nm)	ϵ[b]	$M_r \times 10^{-6}$
0	800	0	37
	900	0.1	37
	975	0.2	37
3.3	600	0	37
	700	0.1	37
5.0	600	0	37
	700	0.1	37
6.6	550	0	37
	650	0.1	37

[a] No ethanol present. $[Na^+]$ = 15 mM. RK2 DNA = 5 μg/mL. Data are fit using only P_{RC} at all magnesium concentrations. Neither collapse nor aggregation occurs.

[b] Several values for R_g and ϵ are compatible with the data at each magnesium concentration because of the uncertainties in the data at this low DNA concentration.

scattering intensity. As the Mg^{2+} concentration was increased and the DNA underwent the transition from an expanded coil to a compact particle, angular measurements became possible, but still had a large amount of error. Nonetheless, the increase in the compact-spherelike contribution to the scattering with increasing Mg^{2+} concentration, eventually attaining aggregation, was still obvious even at these low DNA concentrations (Fig. 4).

A comparison of the range of Mg^{2+} concentration of the two-component region to the Mg^{2+} dependence of a 90° scattering profile is of interest. The two-component behavior was found to begin at Mg^{2+} concentrations below those giving the pronounced increase in the 90° intensity when the DNA concentration is less than 1.0 μg/mL. Thus, at low DNA concentration, any easily detected increase in scattering at 90°, above the background due to solvent, is the result of aggregation. At 9.9 μg/mL of DNA, a rise in the 90° scattering was observed before aggregation, but only after a large population of condensed molecules had formed. The single-angle behavior at a low DNA concentration (0.6 μg/mL) and at a high DNA concentration (9.9 μg/mL) is shown in Fig. 5, with the two-component region indicated by the broken line. The values of f in this region are listed in Table II. The two-component region falls at the beginning of the transition defined by a rise in the intensity at a single angle and represents only a small fraction of the total increase. Further increase in the 90° scattering at magnesium concentrations greater than those of the two-component region is a result of aggregation. (Had the full 90° profile been measured for the 9.9 μg/mL sample, the 90° intensity expected for the plateau region would have been 15–20 times the largest intensity shown in Fig. 5.)

The transition to compact particles occurred over a period of several hours. The scattering intensity often required 4–7 h after the addition of

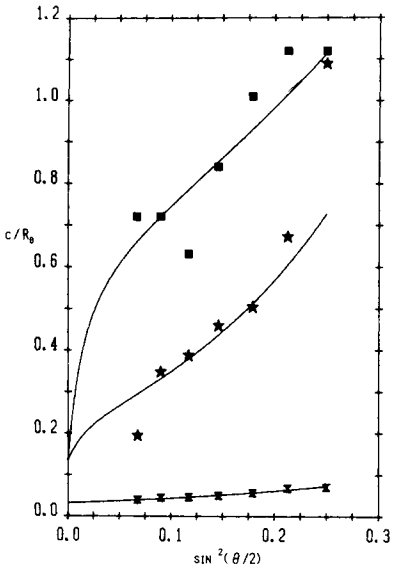

Fig. 4. Reciprocal-intensity plot of RK2 DNA at low concentration in ethanol–water solvent. Magnesium is added to a concentration high enough to produce aggregation. RK2 DNA, 0.6 μg/mL, 25% by weight ethanol, 11 m*M* Na^+. Symbols are as follows:

	$[Mg^{2+}]$	f	R_g	R	$M_r \times 10^{-6}$
■	4.3 m*M*	0.80	975 nm	125 nm	37
★	4.9	0.45	600	175	37
x	5.2	0	—	150	160

an aliquot of Mg^{2+} before no further change in intensity was observed over a 1-h period. An example of the change with time in the scattering intensity and angular dependence is shown in Fig. 6. The solution had not stabilized after 3.5 h. As the reciprocal-intensity decreased, the slope of the curve became smaller, consistent with an increase in the fraction of small spherelike particles.

Reversibility of the Collapsed State

Measurement of a phase diagram requires reaching a thermodynamically stable state; faithful reversibility of the transition must be demonstrated. Hysteresis has been noted by Dore and coworkers[15] in the condensation of T2 DNA at low pH and by Widom and Baldwin[16] in the cobalt–hexamine-induced transition of DNA from λ phage. In this work hysteresis was also found, but only with samples in which large aggregates had formed. If the collapsing agent was added only to a level at which a large fraction of the DNA was collapsed, with a small fraction of the DNA still in an expanded structure (*i.e.*, $0 < f < 0.5$ and $M_r = 37 \times 10^6$), and the reaction was then reversed and left for several hours, no hysteresis was observed. The experiments are described in this section.

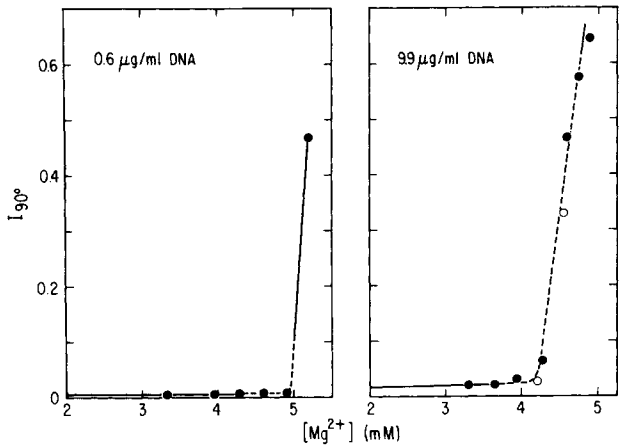

Fig. 5. The 90° scattering intensity from RK2 DNA in ethanol–water solvent as a function of magnesium concentration. The dashed line indicates the region in which the angular dependence of scattering contains contributions from two components, as shown by the parameters listed in Table II. Conditions: 25% by weight ethanol, 11 m*M* Na^+. Filled circles (●) are for the forward reaction by titration with magnesium; open circles (○) are for the reverse reaction by titration with EDTA.

Initial investigations of hysteresis involved reversing the spermidine-induced condensation of T7 DNA by dilution of the sample with buffer. The samples were extensively aggregated as judged by a 90° intensity several times greater than that expected for the zero-angle intensity. A return to near the original scattering level as observed but with a large hysteresis. In contrast to the increase in scattering occurring between 40 and 45 μ*M* spermidine, the decrease did not appear until 22–27 μ*M* spermidine.

A condensing reagent more convenient for examining the problem of hysteresis is Mg^{2+} in ethanol–water solution. The concentration of free Mg^{2+} can be easily reduced by addition of the chelating agent ethylene diamine tetraacetic acid (EDTA). As with spermidine-compacted T7 DNA, if RK2 DNA samples were titrated to a Mg^{2+} concentration high enough to induce substantial aggregation, hysteresis was observed. The transition in the 90° scattering intensity occurred at Mg^{2+} concentrations that differ in the forward and reverse reaction by 0.2–0.6 m*M* out of approximately 4.0 m*M*.

Other experiments involved limited titrations, increasing the Mg^{2+} concentration only to the level at which a substantial fraction of the DNA was collapsed, and reversing condensation with EDTA before the start of aggregation. That a fraction of the DNA was collapsed is indicated by a decrease in the angular dependence of scattering, while the intensity at all angles remained less than the expected zero-angle intensity. Following this titration procedure, the 90° scattering was identical for both the forward and reverse transition, as shown in Fig. 5(b) ([DNA] = 9.9 μg/mL; open circles mark the intensity measured for the reverse reaction). Nor

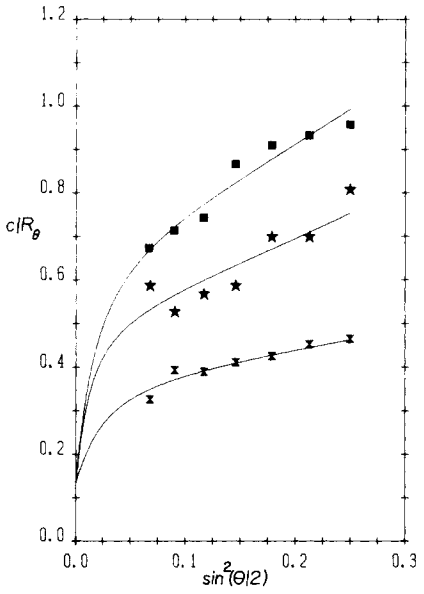

Fig. 6. Time dependence of the collapse transition. Reciprocal-intensity plots of the light-scattering data from RK2 DNA (2.0 μg/mL, 25% by weight ethanol, 11 m*M* Na^+, 4.9 m*M* Mg^{2+}) at different times after the increase in magnesium from 4.6 to 4.9 m*M*.

	f	R_g	*R*	Time
■	0.82	925 nm	100 nm	0.5 h
★	0.75	975	100	3.5
⧗	0.68	600	75	23.0

did the angular dependence of scattering resulting from collapse show hysteresis. The values for R_g, R, and f determined for both the forward and reverse transition are shown in Table II (RK2 [DNA] = 2.0, 5.0 and 9.9 μg/mL). The free Mg^{2+} concentration for the reverse reaction is reported as [Mg^{2+}]-[EDTA]. R_g, R, and f are equivalent in both directions. The corresponding reciprocal-intensity plots of both the calculated curves and the observed data from RK2 DNA, 2 μg/mL, are shown in Fig. 7.

CONCLUSIONS

Collapse Transition of DNA

Probably our most striking result is the finding of two coexisting populations of DNA—a compact sphere and an extended random coil—with the fraction of the DNA concentration in the collapsed state increasing with the concentration of magnesium (see Table II). (This result was a surprise to us and is not suggested by most of the previous literature, but it was clearly anticipated by Gosule and Schellman in their flow-dichroism studies.[5]) The two-component behavior of RK2 DNA existed over a nar-

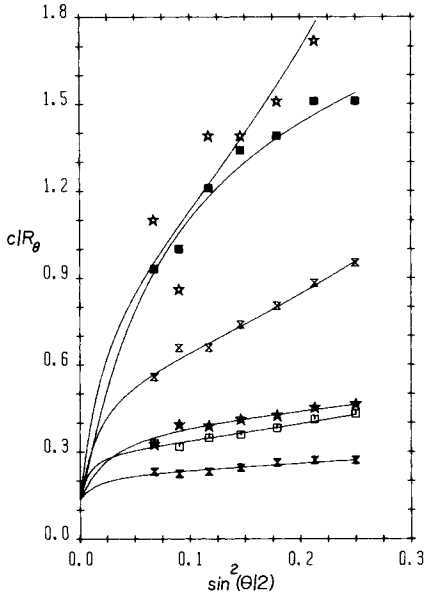

Fig. 7. Light-scattering plots of the magnesium-induced collapse of RK2 DNA in ethanol–water solvent, for both the forward (filled symbols) and reverse (unfilled symbols) reactions. Data were taken for 2.0 μg/mL RK2 DNA, 25% by weight ethanol, 11 m*M* Na^+. The data were fit with the monomolecular value $M_r = 37 \times 10^6$ and with the following values for f, R_g, and R (which also appear in Table II):

	$[Mg^{2+}]$	$[Mg^{2+}]$-[EDTA]	f	R_g	R
☆		4.5 m*M*	0.87	975 nm	150 nm
■	4.6 m*M*		0.93	700	50
⧗		4.7	0.77	875	125
★	4.9		0.68	600	75
□		4.9	0.55	975	100
⧗	5.2		0.41	600	75

row range in magnesium concentration, varying from about 10 to 25% of the total, corresponding presumably to a narrow range of χ. The scattering from a sample titrated to the two-component region could be reversed to the initial low-intensity, large-angular-dependence profile without hysteresis, indicating that the two-component state was thermodynamically stable, or at least metastable.

The two-component populations of DNA might represent a Boltzmann distribution of molecules between two states with approximately equal free energies. We do not know whether an individual DNA molecule rapidly converts between the collapsed and expanded states, or whether the conversion is slow; however, the data of Fig. 6 suggest that it is slow. Although the two-component region has been discussed here in terms of two configurations for a given molecule, we must also note that the data are not inconsistent with a single molecule being partially collapsed and partially expanded.

Some samples were titrated beyond the two-component region, but aggregation resulted, as indicated by intensities at small angles that exceeded the maximum, zero-angle intensity for monomolecular RK2 DNA [see curve (⧗) in Fig. 4]. The scattering data from the aggregated samples could be fit with a single scattering function for a sphere with M_r greater than 37×10^6. Dissociation from the aggregated state occurred with hysteresis.

Although a significant fraction of the DNA collapses before aggregation occurs, a solution of all monomolecularly collapsed DNA (i.e., $f = 0$ and $M_r = 37 \times 10^6$) was found for only one sample. Thus, at these DNA concentrations, the collapse region does not extend over a broad range in magnesium concentrations (and χ), precipitation beginning before or at the completion of the thermally broadened collapse transition. The one sample in Table II (9.9 μg/mL and 5.2 mM [Mg^{2+}]) in which all the DNA appeared to be monomolecularly collapsed was kept under those solvent conditions for only 4 h, a time perhaps too short to establish stability against aggregation.

A quantitative comparison of the theoretical phase diagram in the preceding paper[1] with the light-scattering data of Table II is possible. For a molecular weight of 37×10^6, the theory predicts that the highest DNA concentration within the collapse region is between 0.5 and 1.0 μg/mL. On the other hand, the data collected for RK2 DNA show that the collapse transition, as indicated by the two-component region, appears at DNA concentrations as high as 9.9 μg/mL. Examination of Fig. 2 in Ref. 1 shows that this discrepancy cannot be resolved by varying the parameter N, since the value of log[DNA] at which the horizontal line at χ_{col} intersects the coexistence curve is unaffected by the choice of N. Thus, the theory does not agree quantitatively with the data. However, in view of the many simplified features of the theory, this disagreement is hardly unexpected.

Comparison of the Collapse of DNA and Synthetic Polymers

The reduction in R_g of synthetic polymers in poor solvents has been measured[23-28] (many other references are also given in Ref. 28). Most synthetic polymers are considerably more flexible than DNA, and according to the single-molecule theory,[2] they are not expected to show two minima in the free-energy function corresponding to distinct expanded and collapsed states in the transition region. The decrease in R_g when the solvent gets poorer should be gradual and continuous. In contrast, a stiff chain such as DNA should have two minima in the free-energy function and should collapse by a transition from one minimum to the other. However, a quantity such as R_g, which is averaged over the whole solution, should still change continuously with χ, since the fraction of molecules, f, in one of the minima changes continuously with χ. Thus, to distinguish the two cases it becomes necessary to look for the coexistence of collapsed and ex-

panded forms. With light scattering this means looking for a composite curve in the angular dependence.

A considerable amount of data on the collapse of polystyrene in cyclohexane solution as the temperature is lowered has been published,[24-27] but there is no report of a composite angular-dependence curve. Angular-dependence curves are presented by Sun et al.[26]; these appear to correspond to single random coils all the way through the transition, in at least qualitative accord with our theory.[2]

DNA Concentration Dependence of the Transition in Poor Solvent

The phase diagram, derived from a simple mean-field theory of polymer solutions,[1] predicts that the collapse transition might be differentiated from aggregation by the different dependences of the two transitions on polymer concentration. We attempted to measure the concentration dependence of both transitions by establishing the transition points from an increase in the scattered intensity at a single angle; however, this method did not work well. Of the two transitions, only aggregation was easily detectable at 90° at the low concentrations that were necessary. Moreover, neither spermidine-induced aggregation nor magnesium-induced aggregation occurred with any substantial dependence on DNA concentration for the range of about 0.3–10 μg/mL in [DNA]; thus, trying to distinguish the two transitions with this method is difficult. We do not actually have a theoretical prediction of the extent of the DNA concentration dependence on either spermidine or magnesium concentration, since the quantitative relationship between their concentrations and χ is not known.

Our light-scattering results are in contrast with the observations of other workers who found that condensation at higher DNA concentrations required larger amounts of both spermidine[5] and hexamine–cobalt.[16] This direction of the dependence is not predicted by the theory.[1] Collapse is expected to occur in poor solvents with no DNA concentration dependence, and aggregation should occur at *lower* concentrations of condensing reagent at higher DNA concentrations since, on the left side of the theoretical phase diagram, the two-phase boundary is crossed at smaller χ for higher concentrations of polymer.

This work was supported in part by GM-11916 and by an IBM Graduate Fellowship awarded to C.B.P.

References

1. Post, C. B. & Zimm, B. H. (1981) *Biopolymers* **21,** 2123–2137.
2. Post, C. B. & Zimm, B. H. (1979) *Biopolymers* **18,** 1487–1501.
3. Wilson, R. W. & Bloomfield, V. A. (1979) *Biochemistry* **18,** 2192–2196.
4. Allison, S. A., Herr, J. C. & Schurr, J. M. (1981) *Biopolymers* **20,** 469–488.
5. Gosule, L. C. & Schellman, J. A. (1978) *J. Mol. Biol.* **121,** 311–326.
6. Wang, F. W. (1971) Ph.D. dissertation, University of California, San Diego.
7. Wang, F. W. & Zimm, B. H. (1981) *Biopolymers* **20,** 1333–1335.

8. Leite, R. C. C., Moore, R. S., Porto, S. P. S. & Ripper, J. E. (1965) *Phys. Rev. Lett.* **14,** 7–9.
9. Massie, H. R. & Zimm, B. H. (1965) *Proc. Natl. Acad. Sci. USA* **54,** 1641–1643.
10. Kolter, R., Inuzuka, M., Figurski, D., Thomas, C., Stalker, D. & Helinski, D. R. (1978) *Cold Spring Harbor Symp. Quantum Biol.* **43,** 91–97.
11. *International Critical Tables of Numerical Data Physics, Chemistry, and Technology,* Vol. 6 (1929) pp. 245, 254.
12. Jackson, E. L. & Rosenthal, S. M. (1960) *J. Org. Chem.* **25,** 1055–1056.
13. Lerman, L. S. (1971) *Proc. Natl. Acad. Sci. USA* **68,** 1886–1890.
14. Jordan, C. F., Lerman L. S., & Venable, J. H., Jr. (1972) *Nature* [*New Biol.*] **236,** 67–70.
15. Dore, E., Frontali, C. & Gratton, E. (1972) *Biopolymers* **11,** 443–459.
16. Widom, J. & Baldwin, R. L. (1980) *J. Mol. Biol.* **144,** 431–453.
17. Harpst, J. A. (1980) *Biophys. Chem.* **11,** 295–302.
18. Borochov, N., Eisenberg, H. & Kam, Z. (1981) *Biopolymers* **20,** 231–235.
19. Zimm, B. H. (1948) *J. Chem. Phys.* **16,** 1099–1116.
20. Schmid, C. W., Rinehart, F. P. & Hearst, J. E. (1971) *Biopolymers* **10,** 883–893.
21. Sharp, P. & Bloomfield, V. A. (1968) *Biopolymers* **6,** 1201–1211.
22. Ross, P. D. & Scruggs, R. L. (1968) *Biopolymers* **6,** 1005–1018.
23. Mazur, J. & McIntyre, D. (1975) *Macromolecules* **8,** 464–476.
24. Slagowski, E., Tsai, B. & McIntyre, D. (1976) *Macromolecules* **9,** 687–688.
25. Nierlich, M., Cotton, J. P. & Farnoux, B. (1978) *J. Chem. Phys.* **69,** 1379–1383.
26. Sun, S. T., Nishio, S. T., Swislow, G. & Tanaka, T. (1980) *J. Chem. Phys.* **73,** 5971–5975.
27. Bauer, D. R. & Ullman, R. (1980) *Macromolecules* **13,** 392– 396.
28. Nishio, I. Sun, S. T., Swislow, G. & Tanaka, T. (1979) *Nature* **281,** 208–209.

Received January 12, 1982
Accepted April 23, 1982